Cosolvent Effects on the Micellization of Oxyphenyl(copoly)ethylene Oxide Copolymers in Aqueous Solution

ARTICLE *in* THE JOURNAL OF PHYSICAL CHEMISTRY B · AUGUST 2006

Impact Factor: 3.3 · DOI: 10.1021/jp061322d · Source: PubMed

3 AUTHORS:

Emilio Castro
Universidad de Sevilla
34 PUBLICATIONS **488** CITATIONS
SEE PROFILE

Pablo Taboada
University of Santiago de Compostela
149 PUBLICATIONS **2,317** CITATIONS
SEE PROFILE

Víctor Mosquera
University of Santiago de Compostela
170 PUBLICATIONS **3,114** CITATIONS
SEE PROFILE

Cosolvent Effects on the Micellization of Oxyphenyl(copoly)ethylene Oxide Copolymers in Aqueous Solution

Emilio Castro, Pablo Taboada,* and Víctor Mosquera

Laboratorio de Física de Coloides y Polímeros, Grupo de Sistemas Complejos, Departamento de Física de la Materia Condensada, Facultad de Física, Universidad de Santiago de Compostela, Spain

Received: March 2, 2006; In Final Form: April 27, 2006

In the present paper, we have analyzed how the presence of ethanol affects the micellization process of two structurally related polyoxyethylene block copolymers with diblock and triblock architectures (diblock, $S_{15}E_{63}$; triblock, $E_{67}S_{15}E_{67}$) and the same hydrophobic block length, formed by oxyphenylethylene units, through surface tension, static and dynamic light scattering, density, ultrasound velocity, transmission electron microscopy, and steady-state fluorescence techniques. E and S denote the oxyethylene ($-OCH_2CH_2$) and oxyphenylethylene ($-OCH_2CH(C_6H_5)$) units, respectively, and the subscripts the block length. The effect of increasing amounts of ethanol in solution gives rise to a progressive disruption of the micelle structures formed by these copolymers, with an increase in the critical micelle concentration (cmc) values and a decrease in the micellar aggregation number. This originated from the deswelling of the poly(ethylene oxide) (PEO) chains due to a decrease of the water content, accompanied by a reduction of the solvophobicity and an increase of the solubility of the S blocks, causing the lowering of the interfacial tension between the polyoxyphenylethylene core and the solvent, and favoring the swelling of hydrophobic blocks. Therefore, to achieve thermodynamic equilibrium, the micelle size should be smaller. A model derived from small angle neutron scattering (SANS) data is also applied to get extra information on micelle structure. With the aim of obtaining information about the hydration of micellar solutions of these block copolymers, compressibility and fluorescence data were collected. The increase of compressibility with ethanol addition confirms the swelling of the hydrophobic polyoxyphenylethylene chains. Fluorescence data show that the addition of ethanol to the solution decreases the polarity, favoring the solubilization of the oxyphenylethylene chains in the mixed solvent as single monomers. Aggregation data derived from this technique are in fair agreement with those obtained from light scattering.

1. Introduction

Polyoxyalkylene amphiphilic copolymers containing both polyoxyethylene hydrophilic block and different hydrophobic blocks are widely used in industrial processes. These copolymers can form self-assembled aggregates when dissolved in a selective solvent,[1] from spherical micelles in dilute solutions (with a "core" made up of the hydrophobic block and a "corona" composed of the water-soluble polyoxyethylene block) to lyotropic liquid crystals at higher concentrations. The molecular weight and the chemical nature of the copolymer can be adjusted to meet specific requirements of different applications, such as dispersion stabilization, foaming, detergency, emulsification, and pharmaceutical formulations.[2] However, other alternative mechanisms can also be used. In this respect, one of the key factors in determining the behavior of these copolymers in solution is solvent quality. This can be altered either by a change in temperature or by the addition of cosolvents or cosolutes to water. Water is typically used as a solvent for amphiphilic block copolymers. The addition to water of polar cosolvents provides an extra degree of freedom in tailoring the solution properties for specific applications such as in pharmaceutical formulations of non-water-soluble drugs and cosmetics that employ copolymers as excipients or carriers,[3] in water-based inks used in ink-jet printers,[4] or as templates in mesoporous silica formation.[5]

In the past decade, a great deal of effort has been devoted to the study of the physicochemical properties and nanostructure formation of polyoxyethylene-based block copolymers in different solvents and mixed solvents, mainly on those whose hydrophobic block is formed by polypropylene oxide (denoted as P or PPO), known as Pluronics, Synperonics, or polaxamers. It has been demonstrated that solvent quality is a controllable factor in the critical micelle concentration (cmc), critical micelle temperature (cmt), and structure of their micelles and lyotropic crystals.[6−11] However, less attention has been paid to other polyoxyethylene-based block copolymers.[12,13]

To fill this gap, in the present work, we study the micellization properties of two polyoxyethylene block copolymers with the same hydrophobic block length and different molecular architectures (one diblock and another triblock) in mixed solvents formed by water and different amounts of ethanol. Ethanol has been investigated as a cosolvent in solutions of several Pluronic copolymers[8,10,14−19] and for an E/P copolymer with two statistical blocks.[20] For dilute aqueous solutions, addition of ethanol has been found to increase the cmc and cmt of several Pluronic copolymers,[8,10,14−16] consistent with ethanol being a better solvent than water. For concentrated micelle solutions, ethanol increases the critical gelation temperature (cgt).[14,15,17]

The hydrophobic block of both copolymers is formed by polyoxyphenylethylene units ($-OCH_2CH(C_6H_5)$, denoted as S). The molecular formulas of these copolymers are $S_{15}E_{63}$ and

* To whom correspondence should be addressed. E-mail: fmpablo@usc.es. Phone: 0034981563100 Ext. 14042. Fax: 0034981520676.

10.1021/jp061322d CCC: $33.50
Published on Web 06/14/2006

TABLE 1: Molecular Characteristics of the Copolymer[a]

	M_n (g mol^{-1}) (NMR)	wt % S (NMR)	M_w/M_n (GPC)	M_w (g mol^{-1})
$E_{67}S_{15}E_{67}$	7700	23.0	1.04	8000
$S_{15}E_{63}$	4600	39.7	1.04	4780

[a] Estimated uncertainty: M_n to ±3%; wt % S to ±1%, M_w/M_n to ±0.01. M_w calculated from M_n and M_w/M_n.

$E_{67}S_{15}E_{67}$ for the diblock and triblock copolymer, respectively, where E denotes the oxyethylene unit ($-OCH_2CH_2$) and the subscripts denote the length of each block. The synthesis and micellization properties in water of both block copolymers have been previously reported.[21,22] It has been demonstrated[21] that the hydrophobicity of the styrene oxide block based on the cmc if compared with those of propylene and butylene oxide (B) blocks is in the ratio P/B/S = 1:6:12. Moreover, it has been shown that the lower glass transition of poly(styrene oxide) ($T_g \approx 40$ °C) compared to that of poly(styrene) ($T_g \approx 100$ °C) means that effects caused by the immobility of blocks in the micelle core are less important in micellar solutions of this class of copolymers, providing sufficient mobility to readily solubilized aromatic drugs.[23]

2. Experimental Section

Materials. The synthesis of the copolymers was described previously in detail.[21,22] Table 1 shows the molecular characteristics of both copolymers. Water was double distilled and degassed before use. Ethanol was of Analar grade. Pyrene and DMA were purchased from Sigma Chemical Co.

Surface Tension Measurements. Surface tensions (γ) of the triblock copolymer $E_{67}S_{15}E_{67}$ were measured by the Wilhelmy plate method using a Krüss K-12 surface tension instrument, equipped with a processor to acquire the data automatically. The equipment was connected to a circulating water bath to keep the temperature constant at 20 °C to within ±0.01°C. The plate was cleaned by washing with doubly distilled water followed by heating in an alcohol flame. A stock solution (1.0 g dm^{-3}) was prepared with distilled water and diluted as required. In the measurements, a solution was equilibrated at 20 °C and the surface tension was recorded at 15 min intervals until a constant value was reached, a process which took 12−36 h depending on concentration. The accuracy of the measurements was checked by frequent determination of the surface tension of pure water.

Light Scattering Measurements. Dynamic and static light scattering (DLS and SLS) intensities were measured for solutions at 20 °C by means of an ALV-5000F (ALV-GmbH, Germany) instrument with vertically polarized incident light of wavelength $\lambda = 532$ nm supplied by a continuous wave (CW) diode-pumped Nd:YAG solid-state laser supplied by Coherent Inc., CA, and operated at 400 mW. The intensity scale was calibrated against scattering from toluene. Measurements were made at a scattering angle of $\theta = 90°$ to the incident beam. Solutions were equilibrated at each chosen temperature for 30 min before making a measurement. Experiment duration was in the range 3−5 min, and each experiment was repeated two or more times. All solutions were optically clear to the eye. They were clarified by filtering through Millipore Millex filters (Triton free, 0.22 μm porosity) directly into the cleaned scattering cell.

The correlation functions from DLS were analyzed by the CONTIN method to obtain the intensity distributions of decay rates (Γ).[24] The decay rate distributions gave the distributions of the apparent diffusion coefficient ($D_{app} = \Gamma/q^2$, $q = (4\pi n_s/\lambda)\sin(\theta/2)$, n_s = refractive index of solvent), and integrating over the intensity distribution gave the intensity-weighted average of D_{app}. Values of the apparent hydrodynamic radius ($r_{h,app}$, radius of a hydrodynamically equivalent hard sphere corresponding to D_{app}) were calculated from the Stokes−Einstein equation

$$r_{h,app} = kT/(6\pi\eta D_{app}) \quad (1)$$

where k is the Boltzmann constant and η is the viscosity of water at temperature T.

The basis for analysis of SLS was the Debye equation

$$K^*c/(I - I_s) = (1/M_w) + 2A_2c + ... \quad (2)$$

where I is the intensity of light scattering from solution relative to that from toluene, I_s is the corresponding quantity for the solvent, c is the concentration (in g dm^{-3}), M_w is the mass-average molar mass of the solute, A_2 is the second virial coefficient (with higher coefficients being neglected), and K^* is the appropriate optical constant which includes the specific refractive index increment, dn/dc.[21,22] Other quantities used were the Rayleigh ratio of toluene for vertically polarized light, $R_v = 2.57 \times 10^{-5}[1 + 3.68 \times 10^{-3}(t - 25)]$ cm^{-1} (t in °C), and the refractive index of toluene,[25] $n = 1.4969[1 - 5.7 \times 10^{-4}(t - 20)]$. The possible effect of the different refractive indices of the blocks on the derived molar masses of micelles has been considered for E_mS_n copolymers and found to be negligible.[26]

Transmission Electron Microscopy (TEM). Samples for transmission electron microscopy were prepared by evaporation of a 2.5 g dm^{-3} aqueous micellized copolymer solution of different ethanol solutions negatively stained with 2% phosphotungstic acid (wt/vol) under air. A drop of copolymer solution was placed on an electron microscope copper grid. After drying, electron micrographs of the sample were obtained with a Phillips CM-12 electron microscope.

Density and Ultrasound Velocity Measurements. Density and ultrasound velocity measurements were carried out at 20 °C using a commercial density and ultrasound velocity measurement apparatus (Anton Paar DSA 5000 densimeter and sound velocity analyzer) equipped with a new generation stainless steel cell. One of the principal limitations of custom-built systems resides in possible temperature drifts. This problem was circumvented in the present study by maintaining the temperature control by the Peltier effect, giving a resolution of ±0.001 °C and uncertainties in density of ca. $\pm 1 \times 10^{-6}$ g cm^{-3}. Errors in ultrasound velocity measurements also arise mainly from variations of temperature, and in this study, the resolution was ±0.01 m s^{-1}. The densimeter and the ultrasound equipment were calibrated using deionized and doubly distilled water and air, whose densities and velocities were compared from literature ones.[26]

For a nonscattering system, there is a simple relationship between the ultrasonic velocity of a solution and its physical properties. Assuming that the wavelength of sound is much greater than the particle size and independent of the frequency, the adiabatic compressibilities of sample solution (β) and solvent (β_0) can be calculated using the Laplace equation,[27] $\beta = 1/(\rho u^2)$, with a sound velocity (u) and density (ρ) data set of the sample solution. The isentropic compressibility coefficient is expressed in bar^{-1} when u is expressed in cm s^{-1} and ρ is expressed in g cm^{-3}. The adiabatic specific compressibility (β_S) of the copolymer $S_{15}E_{63}$ was calculated using eq 3 at temperatures of 20, 30, and 40 °C[28]

$$\beta_S = -\frac{1}{v}\left(\frac{\partial v}{\partial p}\right)_S = \left(\frac{\beta_0}{vc}\right)\left[\frac{\beta}{\beta_0} - \frac{\rho - c}{\rho_0}\right] \quad (3)$$

where p is the pressure and c is the concentration of the solute (copolymer) in g cm^{-3}, β_0 is the solvent mixture density, and v is the partial specific volume, which can be determined from density measurements using the relation $v = 1/\rho_0(1 - (d\rho/dc))$.

Fluorescence Measurements. Fluorescence measurements were recorded on a Spex Fluoromax-2 spectrofluorometer in the "S" mode with band-passes for excitation and emission monochromators of 1.05 nm. This apparatus is equipped with a thermostated cell housing, fitted with a 150 W xenon lamp and 1 cm × 1 cm quartz cells. λ_{exc} was 339 nm, and the averaged (during 60 s) fluorescence intensities were recorded at the maximum first and third vibronic pyrene peaks at 20 °C.

The pyrene 1:3 ratio index was used to obtain information on the micellar micropolarity changes induced by the presence of ethanol in the solvent system. To determine the aggregation numbers from steady-state fluorescence measurements, the addition of a quencher is required. In our case, DMA was used. The experimental results were analyzed by the Turro and Yekta model[29]

$$\ln(I/I_0) = [Q_t]/[M] \quad (4)$$

In this equation, [M] is the concentration of micelles given by

$$[M] = \frac{[\text{copolymer}] - \text{cmc}}{N} \quad (5)$$

I_0 and I are the fluorescence intensities at zero and $[Q_t]$ concentrations of the quencher, and N is the aggregation number of the copolymer micelle. Equation 5 is derived under the following assumptions: (a) the quencher and the fluorescence probe are entirely in the micellar phase, (b) the distributions of the quencher and the probe obey Poisson statistics, and (c) the probe only fluoresces in the absence of quencher.

3 Results and Discussion

3.1. Thermodynamics of Micellization. We have studied the micellar formation process of the triblock copolymer $E_{67}S_{15}E_{67}$ in different ethanol−water mixtures by determining the corresponding critical micelle concentration (cmc) values. For this purpose, we have employed the surface tension technique. Representative plots showing several results of these experiments are presented in Figure 1. Previous determination of the cmc of this copolymer in water can be found in ref 22. Extrapolation of the variation of the cmc values with temperature obtained by this technique at 20 °C gave a value of 0.027 g dm^{-3}. The concentration at which the surface tension reached a steady value served to define the cmc. Values are shown in Table 2. Similar experiments were not done for the diblock copolymer $S_{15}E_{63}$ because their cmc values are still too low in the presence of ethanol to be measured with reasonable confidence. From cmc data, it can be inferred that micelles are formed at higher concentrations when ethanol is added to water. This indicates that the ethanol−water mixed solvent becomes a better solvent for the copolymer than pure water. The same trend was observed for Pluronic copolymers.[8,10,14−16] Therefore, the larger cmc values as the content of ethanol increases indicate that the cosolvent is acting as a structure-breaking agent, decreasing the solvophobic effect and favoring the solution of the copolymer in the mixed solvents.

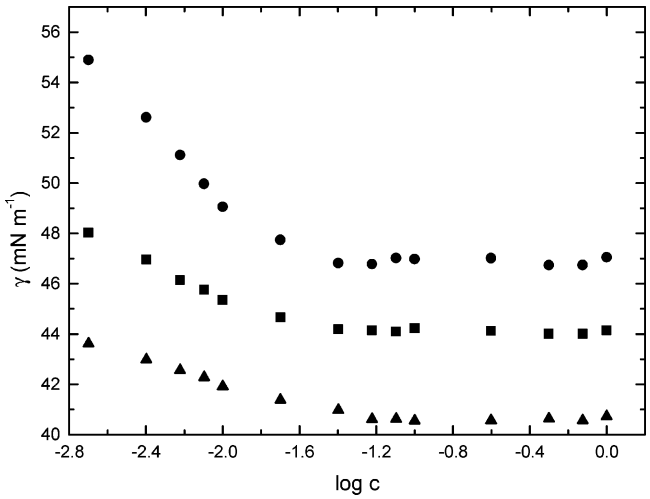

Figure 1. Surface tension (γ) against the logarithm of concentration (in g dm^{-3}) for the triblock copolymer $E_{67}S_{15}E_{67}$ in (●) 5%, (■) 15%, and (▲) 25% (v/v) ethanol in aqueous solution at 20 °C.

According to the mass action model, the standard Gibbs energy of micelle formation per mole of monomer (ΔG°_{mic}) is given by

$$\Delta G^\circ_{mic} = RT \ln x_{cmc} \quad (6)$$

where x_{cmc} is the mole fraction of copolymer at the cmc. The effect of the cosolvent on the micelle aggregation process can be evaluated by means of the so-called Gibbs free energy of transfer (ΔG°_M) which is defined by

$$\Delta G^\circ_M = (\Delta G^\circ_{mic})_{ethanol+water} - (\Delta G^\circ_{mic})_{water} \quad (7)$$

The thermodynamic parameters obtained through eqs 6 and 7 are also listed in Table 2. It is observed that the Gibbs energies of micellization are negative but become lower (in absolute values) as the ethanol content increases. This indicates that the micellization process becomes less spontaneous with the presence of the cosolvent and reflects the role of the ethanol reducing the solvophobic effect, which is considered to be responsible for the micellar formation process, as a consequence of the reduction of solvent cohesive energy due to the increased amounts of ethanol in the solvent mixture. Thus, the chemical structure of the solvent plays an important role in the cohesive energy density.

On the other hand, and as discussed in detail previously,[22] the enthalpy of micellization for this class of copolymers in water with long S blocks is known to be small and positive, which is attributable to the S block being tightly coiled in the dispersed molecular state, so that the interactions of an S unit with water are much reduced in comparison with the interaction enthalpies of the units of copolymers with shorter S blocks, which display a more extended conformation in the molecular state. Thus, the micellization process of long S block copolymers can be assumed safely as entropy driven. However, the progressive addition of ethanol to the solution allows the solvent mixture to be a better solvent for the S blocks, so ethanol is acting as a water structure breaker because its presence disrupts the hydrogen-bond network of water due to the strong interactions between water and ethanol molecules, which results in a less dense coiled packing of these blocks (as will be corroborated in the following section); this involves, as a consequence, a presumable increase in the values of the enthalpy of micellization and, therefore, of the enthalpic contribution to ΔG°_{mic}. Moreover, the values of the free energy of transfer are positive

TABLE 2: Critical Micelle Concentration (cmc), Gibbs Free Energy of Micelle Formation (ΔG°_{mic}), Gibbs Free Energy of Transfer (ΔG°_M), Surface Excess Concentration (Γ_{max}), Minimum Area Per Molecule (A_{min}), and Gibbs Free Energy of Adsorption (ΔG°_{ads}) of the $E_{67}S_{15}E_{67}$ Block Copolymer in Different Aqueous−Ethanol Mixed Solvents at 20 °C[a]

% (v/v)	cmc (g dm^{-3})	ΔG°_{mic} (kJ mol^{-1})	ΔG°_M (kJ mol^{-1})	Γ_{max} (10^{-6} mol m^{-2})	A_{min} (nm^2)	π_{cmc} (mN m^{-1})	ΔG°_{ads} (kJ mol^{-1})
5	0.029	−40.3	0.3	1.23	1.3	46.9	−78.3
15	0.039	−39.6	1.0	0.64	2.6	44.3	−108.3
25	0.055	−38.8	1.8	0.31	5.3	41.1	−168.5

[a] Estimated uncertainties: cmc, ΔG°_{mic}, ΔG°_M, Γ_{max}, and A_{min} to ±10%, π_{cmc} to ±1%, ΔG°_{ads} to ±15%.

and increase with the ethanol content. In particular, this involves the magnitude of the polymer chain transfer Gibbs energy being smaller in pure ethanol than in water and this is the dominant contribution responsible for the observed increase in the cmc as the ethanol content in the solvent mixture increases.

3.2. Thermodynamics of Adsorption. The investigation of the interfacial properties of amphiphilic compounds in solution can provide information about solute−solute and solvent−solute interactions. The surface excess concentration (Γ_{max}) and the minimum area per copolymer molecule (A_{min}) at the air/solvent interface were obtained using the surface tension measurements and the following equations:

$$\Gamma_{max} = -\frac{1}{RT}\left(\frac{\partial\gamma}{\partial \ln c}\right)_{T,p} \quad (8)$$

$$A_{min} = 1/N_A\Gamma_{max} \quad (9)$$

where R is the gas constant, N_A is Avogadro's number, and c is the copolymer concentration. The values of the surface pressure at the cmc (π_{cmc}) were obtained employing the following equation:

$$\pi_{cmc} = \gamma_0 - \gamma_{cmc} \quad (10)$$

The Gibbs free energies of adsorption were obtained through[30]

$$\Delta G^\circ_{ads} = \Delta G^\circ_{mic} - \pi_{cmc}/\Gamma_{max} \quad (11)$$

The standard state in the surface phase is defined as the surface covered with a monolayer of copolymer at the surface pressure equal to zero. The last term in eq 11 expresses work involved in transferring the polymer molecule from a monolayer at zero surface pressure to the micelle.

The values of these adsorption quantities are also shown in Table 2. In the presence of ethanol, the value of Γ_{max} decreases with increasing ethanol content. This decrease can be attributed to several factors, namely, (a) a change in the water structure due to the addition of ethanol, (b) the interaction between the alcohol and the copolymer, and (c) the presence of ethanol at the interface.[31] π_{cmc} also decreases with increasing ethanol concentration in the mixed solvent. In relation to solvent−solvent interactions, binary aqueous mixtures can be classified into three groups according to their excess molar thermodynamic functions of mixing.[32] The water−ethanol mixture belongs to the typically nonaqueous negative group.[33] This group is characterized by a negative excess Gibbs energy (ΔG^{exc}, with $|\Delta H^{exc}| > |T\Delta S^{exc}|$), and ethanol is considered as a structure breaker, as mentioned before. In regard to the solvent−polymer interactions, an increase in the ethanol concentration results in a decrease in the dielectric constant, in the Reichardt parameter (E_T), or in the π^* polarity index[34] of the mixture, this confirming that the bulk phase will be a better solvent for the polymer molecules and their tendency to be adsorbed at the interface will decrease. As a consequence, the surface excess concentration decreases and the minimum area per molecule at the air/mixture interface increases upon increasing the amount of ethanol in the solvent mixture.

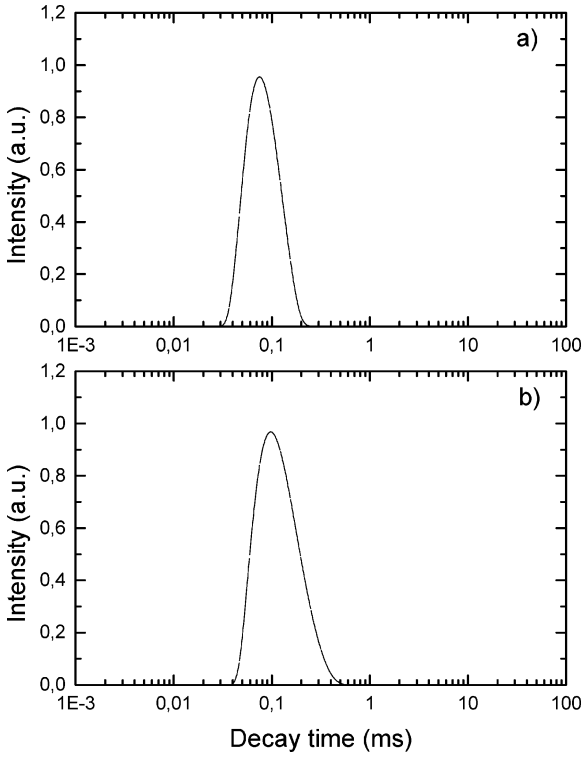

Figure 2. Decay time distributions of diblock $S_{15}E_{63}$ copolymer at a concentration of 80 g dm^{-3} in aqueous solution with an ethanol content of (a) 5% (v/v) and (b) 25% (v/v) at 20 °C.

The values of ΔG°_{ads} become more negative as the ethanol content increases, probably indicating a dehydration of the polyoxyethylene units due to the presence of ethanol molecules. Besides, ΔG°_{ads} values are more negative than their corresponding ΔG°_{mic} values. This points out that, when a polymer micelle is formed, work has to be done to transfer the polymer molecules in the monomeric state at the surface to the micellar stage through the aquous medium.[35]

3.3. Micellar Parameters. We performed experiments at copolymer concentrations well above the cmc for the different compositions of the mixed solvents to allow the measurements of the micelle sizes.

The intensity fraction distributions of decay times from DLS measurements obtained for copolymers $E_{67}S_{15}E_{67}$ and $S_{15}E_{63}$ contained narrow peaks and were assigned to spherical micelles formed by a closed association process. The decay time distribution of copolymer micelles in mixed solvents slightly widens as the ethanol content in the solvent increases, as seen in Figure 2 for the diblock copolymer.

As can be seen in Figure 3, the apparent diffusion coefficient is an increasing linear function of the copolymer concentration. The positive slopes of the plots in this figure are consistent with the micelles acting effectively as hard spheres.

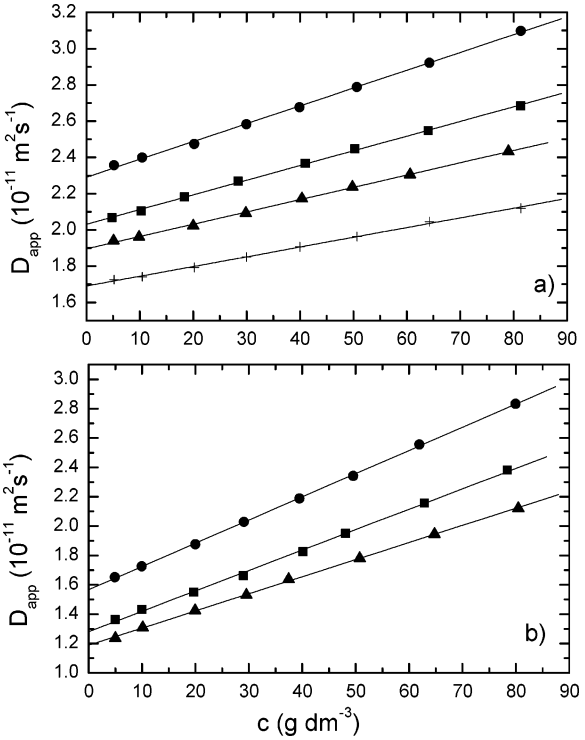

Figure 3. Apparent diffusion coefficients of copolymers (a) $E_{67}S_{15}E_{67}$ and (b) $S_{15}E_{63}$ in the presence of aqueous solutions with (●) 5% (v/v), (■) 10% (v/v), (▲) 15% (v/v), and (+) 25% (v/v) ethanol at 20 °C.

TABLE 3: Micelle Properties of $S_{15}E_{63}$ and $E_{67}S_{15}E_{67}$ Block Copolymers in Different Aqueous−Ethanol Mixed Solvents at 20 °C[a]

	% (v/v)	D_0 (10^{-11} m^2 s^{-1})	r_h (nm)	M_w (10^5 mol g^{-1})	N_w	δ_t	r_t (nm)	a_t (Å^2)
$S_{15}E_{63}$	0[b]	1.80	11.9	6.6	138	4.8	10.4	947
	5	1.57	11.5	5.9	122	4.9	10.0	1030
	15	1.28	9.9	4.2	87	4.4	8.6	1093
	25	1.19	7.9	2.6	55	3.8	6.9	1088
$E_{67}S_{15}E_{67}$	0[b]	2.61	8.2	1.9	24	3.4	6.1	1948
	5	2.29	7.9	1.7	21	3.2	5.7	1944
	10	2.03	7.5	1.3	16	3.0	5.1	2043
	15	1.90	6.9	1.1	13	2.8	4.6	2046
	25	1.68	5.6	0.8	9	2.3	3.9	2124

[a] Estimated uncertainties to ±5%. [b] Extrapolated at 20 °C.

This behavior is usually accommodated by introducing a diffusion second virial coefficient (k_d) in the equation of the straight line

$$D_{app} = D(1 + k_d c + ...) \quad (12)$$

The coefficient k_d is related to the thermodynamic second virial coefficient (A_2) by[36]

$$k_d = 2A_2M_w - k_f - 2\upsilon \quad (13)$$

where k_f is the friction coefficient and υ is the specific volume of the micelles in solution. As is clear from Figure 3, the positive term in eq 13 is dominant for both copolymers, indicating that the mixed solvent is a good solvent for both block copolymers. Relating A_2 to the effective hard-sphere volume of the micelles (υ_{hs}) ($A_2 = 4N_A\upsilon_{hs}/M_w^2$),[37] it shows that the first term depends on the ratio υ_{hs}/M_w. We have no direct measure of υ_{hs}, but it will be closely related to the hydrodynamic volume. Table 3 shows the apparent diffusion coefficient at infinite dilution (D_0) and the hydrodynamic radii (r_h). The results indicate a reduction of both D_0 and r_h with ethanol concentration, with the decrease in r_h attributed to the increase in solvent viscosity.

To corroborate the results obtained by DLS, we also present a series of TEM images (Figure 4) that follows the evolution of block copolymer micelles of $S_{15}E_{63}$ with changes in the ethanol concentration. It was not possible to follow the evolution of the triblock copolymer by this technique, since the size variations are smaller than those of the diblock and TEM images do not provide enough contrast for this purpose.

Most images of the aggregates are in agreement with size measurements by dynamic light scattering. However, one has to bear in mind that by TEM we image single particles, while DLS gives an average size estimation, which is biased toward the larger-size end of the population distribution. In addition, drying of the solvent during TEM sample preparation also involves removal of solvent in the copolymer corona, reducing the micelle volume. Flow of the dry micelles will flatten micelle spheres, giving rise to a larger cross-sectional area, and, thus, a larger size. Finally, removal of the solvent may induce clusterization of some copolymer micelles due to an increased attraction between them due to a closer approximation between them.[38] Therefore, the TEM measurements must be taken as a semiquantitative approach to the real size of the copolymer micelles.

Nevertheless, TEM images seem to follow the same trends as DLS results, displaying a reduction of the micelle size as the ethanol concentration increases in the mixed solvent. In this respect, Figure 5a shows the image for block copolymer micelles in the presence of 5% ethanol. The average size of the aggregates has been estimated around 25 nm, calculated from the extreme to extreme distance of the spheres (over an average of 100 particles). However, it is also necessary to mention, as well as the precautions mentioned before, that the differing electron densities between the block domains forming the core and the corona of the micelles, respectively, can result in different contrasts of the respective domains, thus altering the measured size.[39] This size is slightly larger than that obtained by DLS measurements due to the possible increase in cross-sectional area. With further addition of ethanol to the solution, there is a decrease in the micelle size, as seen in Figure 5b (ethanol concentration 25%), where the diameter of the particles has been reduced to 18 nm, thus confirming the data from DLS.

This reduction in micelle size can be due to a decrease in the aggregation number and/or a decrease in micellar solvation, as suggested by the ΔG°_{ads} values, which is indicative of the decrease in the driving forces for aggregation. To resolve this question, we combined static light scattering (SLS), compressibility, and fluorescence data.

As noted in the Experimental Section, SLS intensities were usually measured at $\theta = 90°$, as appropriate for particles that are small relative to the wavelength of light. For the present micellar solutions, the dissymmetries (I_{45}/I_{135}) were 1.03 or less, which are consistent with micelles with a small radius of gyration; a maximum value of $r_g \sim 8.9$ and 6.1 nm for the diblock and triblock copolymers, respectively, can be obtained from $r_g = 0.775r_h$ by treating the micelles as uniform spheres.

The Debye equation taken to the second term, A_2, could not be used to analyze the SLS data, as micellar interaction causes curvature of the Debye plot across the concentration range investigated. This feature is illustrated in Figure 5, which shows the Debye plots for the diblock and triblock copolymers at selected ethanol concentrations in the mixed solvent.

The fitting procedure used for the curves was based on a scattering theory for hard spheres[40] whereby the interparticle

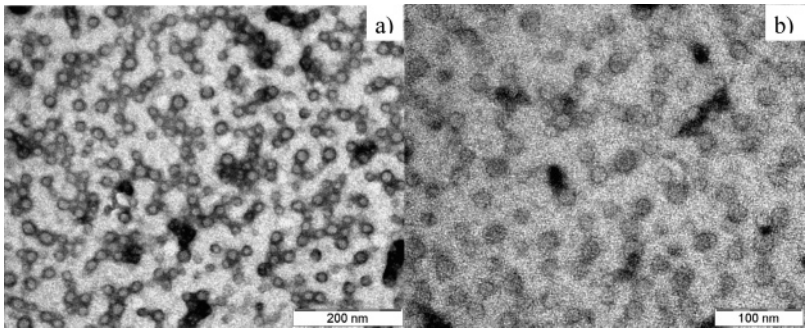

Figure 4. TEM images demonstrating the evolution of triblock copolymer micelle size (copolymer concentration 25 g dm^{-3}) in the presence of (a) 5% (v/v) and (b) 25% (v/v) ethanol.

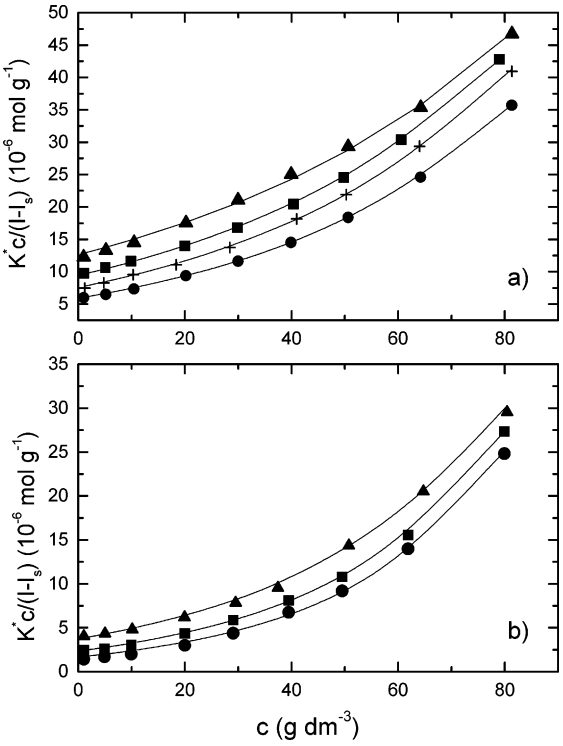

Figure 5. Debye plots of (a) $S_{15}E_{63}$ and (b) $E_{67}S_{15}E_{67}$ in aqueous solutions with an ethanol content of (●) 5% (v/v), (+) 10% (v/v), (■) 15% (v/v), and (▲) 25% (v/v) at 20 °C.

interference factor (structure factor (S)) in the scattering equation

$$K^*c/(I - I_s) = 1/SM_w \qquad (14)$$

was approximated by

$$1/S = [(1 + 2\phi)^2 - \phi^2(4\phi - \phi^2)](1 - \phi)^{-4} \qquad (15)$$

where ϕ is the volume fraction of equivalent uniform spheres. Values of ϕ were conveniently calculated from the volume fraction of copolymer in the system by applying a thermodynamic expansion factor, $\delta_t = \upsilon_t/\upsilon_a$, where υ_t is the thermodynamic volume of a micelle (i.e., one-eighth of the volume (u) excluded by one micelle to another) and υ_a is the anhydrous volume of a micelle ($\upsilon_a = \upsilon M_w/N_{A)}$, where υ is the partial specific volume of the copolymer solute. The fitting parameter (δ_t) applies as an effective parameter for compact micelles irrespective of their exact structure. The method is equivalent to using the virial expansion for the structure factor of effective hard spheres taken to its seventh term[40] but requires just two adjustable parameters, that is, M_w and δ_t.

TABLE 4: Partial Specific Volumes (υ) of Block Copolymers in Different Aqueous−Ethanol Mixtures at 20 °C[a]

	% (v/v)	υ ($cm^3\ g^{-1}$)
$S_{15}E_{63}$	5	0.880
	15	0.871
	25	0.854
$E_{67}S_{15}E_{67}$	5	0.846
	10	0.841
	15	0.835
	25	0.818

[a] Estimated uncertainties to ±5%.

Weight-average association numbers (N_w) are listed in Table 3. These were calculated using values of M_w for the micelles found from the intercepts of the Debye plots and the values of M_w listed for the copolymers in the unimer state in Table 1. The values of N_w decrease as the ethanol concentration in the mixed solvent increases. Values of the thermodynamic expansion factor and the equivalent hard-sphere radius (the thermodynamic radius (r_t)) calculated from the thermodynamic volume of the micelles, that is, from $\upsilon_t = \delta_t\upsilon_a$, are also listed in Table 3. To obtain these data, density measurements of copolymer solutions of varying concentrations were made in media of different ethanol contents. In Table 4, we summarize the results of our density measurements.

To corroborate the aggregation numbers of the triblock copolymer micelles derived from DLS data, we have obtained this micelle parameter from fluorescence quenching experiments, following the procedure developed by Turro and Yekta,[29] which was previously mentioned. This method could not be applied for the diblock because of the low cmc values of this copolymer, which cannot be obtained without significant uncertainties, as mentioned previously. Figure 6 shows representative quenching plots in solution containing a copolymer concentration of 25 g dm^{-3} in aqueous solutions containing different amounts of ethanol. In all cases, we have found a linear behavior. However, we have noted a certain increase in the scattering of experimental points as the ethanol content increases, thus leading to a higher uncertainty in the aggregation number determination. From both the slopes of quenching plots and cmc values, we derived the aggregation numbers listed in Table 5.

It must be noted that the aggregation numbers are in fair agreement with those derived from DLS data, decreasing as the ethanol concentration in the mixed solvent increases.

3.4. Micelle Structure. At this point, it is first necessary to mention again that a possible problem with light scattering is preferential absorption of one component of the binary solvent. When a polymer is dissolved in a binary solvent mixture, eqs 2 and 14 can still be used but considering M_w and A_2 as apparent values.[41] A comparison of the "true" molar mass,

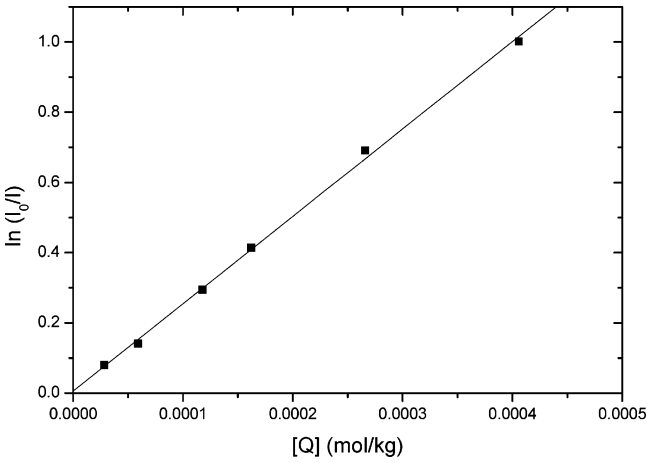

Figure 6. Luminiscence intensity against quencher concentration (DMA) in a 25 g dm^{-3} solution of triblock copolymer $E_{67}S_{15}E_{67}$ at 20 °C.

TABLE 5: Aggregation Numbers of Triblock Copolymer $E_{67}S_{15}E_{67}$ Calculated from Steady-State Fluorescence Quenching Data at 20 °C[a]

% (v/v)	N_w
5	27
10	22
15	12
25	8

[a] Uncertainty in N_w up to ±15%.

as measured in a single solvent, with the apparent molar mass, measured in the solvent mixture, gives the extra contribution to the refractive index due to a preferentially solvating solvent[42]

$$\left(\frac{\partial c_1}{\partial c_0}\right)_{p,T,\mu_j}\left(\frac{\partial n}{\partial c_1}\right)_{p,Y,c_0} = \left(\frac{\partial n}{\partial c_0}\right)_{p,T,c_{j=0}} \times \left[\left(\frac{M_{w,app}}{M_w}\right)^{1/2} - 1\right] \quad (16)$$

where n is the refractive index of the solution, c_0 and c_1 are the concentrations of copolymer and ethanol, respectively, M_w and $M_{w,app}$ are the molecular masses of the copolymers in a single solvent and in the mixture, respectively, and T and p are the temperature and pressure, respectively. If in addition $(\partial n/\partial c_1)_{p,Y,c_0}$ is known, the preferentially solvated solvent can be determined. From the apparent molar masses in Table 3 and eq 16, it follows that the contribution of preferential solvation to the refractive index increment $(\partial c_1/\partial c_0)_{p,T,\mu_j}(\partial n/\partial c_1)_{p,Y,c_0}$ is always positive. On the other hand, it is reasonable to think that $(\partial n/\partial c_1)_{p,Y,c_0}$ is positive in the low ethanol weight fraction region and at not very high copolymer concentrations, so the increment of the refractive index due to the addition of ethanol will predominate; then, it follows that $(\partial c_1/\partial c_0)_{p,T,\mu_j}$ is positive as well. This implies that the copolymers are preferentially solvated by ethanol. However, it is known that preferential solvation cannot be understood on the basis of the solvation properties of the individual solvents; the size of the solvent molecules relative to each other and the affinity of the solvents for each other also play an important role.[43] Thus, further studies would be necessary to exactly determine the extent of preferential absorption. As an estimation, from the values of the molecular masses shown in Table 1, it is expected that at low ethanol concentration preferential adsorption will be low (rough estimations give a value lower than 8%), increasing its importance as the ethanol concentration increases.

In our system, the polyoxyphenylethylene insolubility in water promotes association into micelles, while interactions between poly(ethylene oxide) (PEO) chains oppose it. The addition of ethanol counterbalances the deswelling of the PEO chains due to a decrease of the water content and reduces the solvophobicity and increases the solubility of the S blocks, causing the lowering of the interfacial tension between the polyoxyphenylethylene core and the solvent and favoring the swelling of hydrophobic blocks. Therefore, to achieve thermodynamic equilibrium, the micelle size should be smaller, as shown by the decrease of the hydrodynamic radii for both copolymers as the ethanol concentration increases in the mixed solvent.

This size reduction originated mainly from the reduction in the aggregation number as the ethanol concentration increases, as shown in Table 3, which indicates that the mixed solvent becomes a better solvent for copolymer molecules. This reduction arises from the lowering of the interfacial tension between the hydrophobic core and the mixed solvent, as mentioned previously. Thermodynamic radii (r_t) also diminish with increasing ethanol concentration. Similar behavior has been observed for other block copolymers, such as as $E_mP_nE_m$,[16] or siloxane-graft copolymers.[44] Data in Table 3 show that the aggregation numbers of both copolymers decrease by around ca. 60 and 63% at 25% ethanol whereas the hydrodynamic volume decreases by around 71 and 69% for the same solvent composition for the diblock and triblock, respectively. This fact confirms that size reduction is primarily lead by a decrease in aggregation number. However, the slightly higher reductions in size compared with those of aggregation numbers would indicate that micellar solvation is also changed with the addition of ethanol, as will be discussed in a following section. Variations of both hydrodynamic volume and aggregation number are almost the same up to ethanol concentrations of 15%, so the solvation layer would not be altered much, and only at higher ethanol concentrations, important structural alterations will take place.

On the other hand, it is worth mentioning that the triblock copolymer experiences a little larger reduction in both size and aggregation number as a consequence of the two constraints due to the two block junctions in the core/fringe micellar interface, which involves a less packed micellized structure. Moreover, the reduction of both size and aggregation number is larger for these two block copolymers than for Pluronics in a similar ethanol concentration range. Alexandridis et al.[16] have shown that Pluronic $EO_{37}PO_{58}EO_{37}$ in mixed ethanol−water solvent decreases slightly both the micelle radius and aggregation number up to 20% ethanol, and only at higher alcohol concentration, a strong reduction is observed. In our case, the reduction for both copolymers is more gradual and takes place at lower ethanol content. This can be related to the larger hydrophobicity of the S block if compared to the PO block, which makes the presence of ethanol increase further the solubility of the former block.

To have a more detailed approach to the structure of the block copolymer micelles in the presence of ethanol, we have determined the core radius (r_{core}) and the corona thickness (d) using the model developed by Yang et al.[45] in which the volume fraction of the S block in the core (α_{core}) and of the PEO block in the corona (α_{corona}) is assumed to be different when different cosolvents are present.[16] This approach is based on a core−shell model to fit the small angle neutron scattering (SANS) data from copolymer micelles. In addition, the association number can be calculated. In this model, the association number and the core and corona radii can be related to the volume fraction of S and EO blocks as follows:

$$\alpha_{core} = 3N_w V_S/(4\pi r_{core}^3) \quad (17)$$

$$\alpha_{corona} = 3N_w V_{EO}/[4\pi(r_t^3 - r_{core}^3)] \quad (18)$$

where V_S is the volume of the oxyphenylethylene chains of one copolymer molecule (2.65 nm^3 for both the diblock and triblock), V_{EO} is the volume of ethylene oxide units in one copolymer molecule (4.61 and 9.80 nm^3 for the diblock and triblock copolymers, respectively),[22,46] and r_t is the thermodynamic radius obtained from SLS data. α_{core} and α_{corona} were assumed to be[16] ~1 and ~0.2, respectively; that is, the micellar core has almost no water molecules inside (it is dry) and the corona is highly hydrated. However, it has been demonstrated through SANS data that the amount of water in the propylene and butylene oxide cores of block copolymers is around 20−60 and 50% for propylene[47−49] and butylene oxide,[50,51] respectively. In the case of propylene oxide, it seems that the amount of water in the core depends on the copolymer concentration and solution conditions (temperature, presence of additives, etc.). It would be expected that butylene oxide cores display a lower amount of water in their cores, since their hydrophobicity (based on the molar critical micelle concentration values)[21] is 4 times that of propylene oxide. A reasonable explanation for this fact might be that butylene oxide copolymers used in those studies are terminated by OH groups, thus altering SANS data. Following the same explanation, it would also be expected that styrene oxide should show smaller water core contents than propylene and butylene oxide block copolymers at room temperature, but still displaying a certain amount.

The values of r_{core}, d, and N_w are shown in Table 6. The decrease of r_{core} and d is related to a decrease in the aggregation number, which means that the mixed solvent is a better solvent for the copolymers under study as the ethanol concentration increases. Smaller micelles, with a large part of the hydrophobic chains in contact with the solvent, are unfavorable in water because the interfacial tension between water and the chain is high. The addition of ethanol to water reduces the interfacial tension between the hydrophobic chains and the solvent, and the formation of smaller micelles becomes more energetically favorable, as mentioned previously. Also, note that the association number of the block copolymer micelles derived from this model is higher than the value previously obtained from SLS data as a consequence of the assumptions made during calculations.

On the other hand, it has been demonstrated[16] that the addition of ethanol decreases the volume fractions of Pluronic copolymers both in the core and in the corona, which indicates that both hydrophobic and hydrophilic blocks are solvated to a higher degree. Thus, it would be reasonable to expect that such a behavior will also occur with polyoxyphenylethylene−polyoxyethylene copolymers, with the polyoxyethylene blocks being more hydrophobic. The octanol/water partition coefficient (log P) of ethylene glycol, which has the closest structure to the PEO segments is −1.93; that of styrene oxide is 1.61. Note that a negative log P value indicates that a certain compound, given a choice between water and octanol, prefers to partition to water. The log P value of ethanol is −0.32. Thus, it is more hydrophobic than ethylene glycol and less hydrophobic than styrene oxide. Therefore, addition of ethanol will render it a better solvent for S blocks. As a result, the solvent contents in both the core and the corona of the micelles will increase with an increasing amount of ethanol in the mixed solvent. Moreover, although ethanol is polar and miscible with water, its relative hydrophobicity derives to a higher tendency to mix with the polyoxyphenylethylene chains.

TABLE 6: Modelized Micellization Properties of the $S_{15}E_{63}$ and $E_{67}S_{15}E_{67}$ Block Copolymers in Different Aqueous + Ethanol Mixed Solvents

	% (v/v)	N_w	r_{core} (nm)	d (nm)
$S_{15}E_{63}$	0	199	5.1	5.3
	5	184	4.9	5.1
	15	112	4.2	4.4
	25	55	3.4	3.5
$E_{67}S_{15}E_{67}$	0	40	3.0	3.1
	5	34	2.8	2.9
	10	23	2.5	2.6
	15	17	2.3	2.3
	25	10	1.9	2.0

We have also included in Table 3 the surface area per headgroup (a_t) as determined from the anhydrous radius and the aggregation number by assuming a spherical geometry. This parameter is of considerable interest in the interpretation of the geometric and packing properties of micelles.[52] As seen in the aforementioned table, a_t increases with the presence of ethanol in the solvent mixture. This behavior can be rationalized if we assume that ethanol takes part in the solvation layer of the micelles, by replacing some of the water molecules, resulting in a thicker solvation layer. As a consequence, the steric repulsions between micelles would be increased as the ethanol content increases in the solvent system. In addition, the increase of a_t would impede the growth of micelles, forcing them to adopt spherical shapes.

3.5. Micelle Hydration. To have a more detailed picture of the hydration of copolymer micelles in a mixed ethanol−water solvent, compressibility and pyrene fluorescence measurements were done. As shown previously, the slightly higher reductions in size compared with those of aggregation numbers would indicate that micellar solvation is also changed with the addition of ethanol. If the composition of the solvation layer is modified as a result of the increasing participation of ethanol, it should be reasonable to expect structural alterations in this region of the copolymer micelle. In this respect, two aspects must be considered: first, the effect of steric character, since the ethanol molecule is larger than the water molecule, and, second, the consequence of the minor ability of ethanol to be a hydrogen-bond-forming molecule in relation to water. In this respect, the observed reduction of υ in Table 4 with increasing ethanol content is essentially due to these changes in the micellar solvation status. It must be pointed out that the partial specific volume is affected only by solvent molecules with a significant thermodynamic interaction with copolymer molecules via hydrogen bonds. This aspect is important because it is well-known that PEO chains are strongly hydrated. However, the copolymer micelles can incorporate solvent molecules through two different mechanisms: (a) via hydrogen bonds with ether groups of the PEO chains, which contributes to solvation properly, and (b) by mechanical entrapment in the corona. It has been recently shown[44] that the cosolvent solubility parameter component originating from hydrogen-bonding interactions decreases as the cmc of a siloxane copolymer increases for different water−cosolvent mixtures. This suggests that hydrogen bonding dominates the interactions between water, cosolvent, and polymer. Thus, as the solvent penetration in the core will be larger as the ethanol becomes a better solvent for S chains, as seen by SANS data,[16,47,50] these blocks will become more solvated, thus decreasing the partial specific volume of the copolymer.

An experimental observable sensitive to the hydration properties of solvent-exposed atomic groups as well as the structural properties of polymers[53,54] and biopolymers[55,56] is the specific

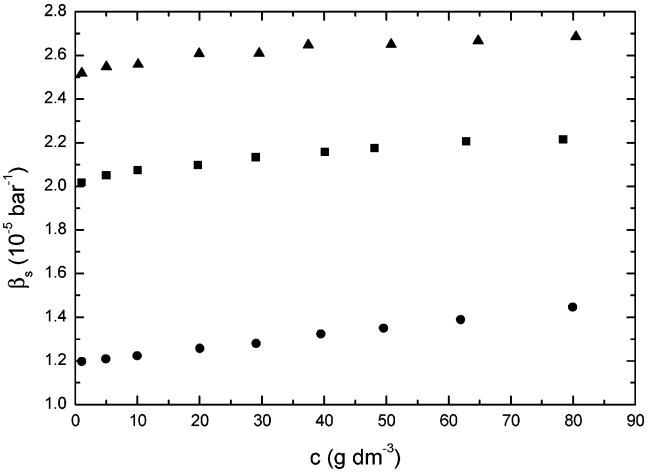

Figure 7. Specific adiabatic compressibility (β_S) as a function of copolymer concentration of $S_{15}E_{63}$ in aqueous solution with an ethanol content of (●) 5% (v/v), (■) 15% (v/v), and (▲) 25% (v/v) at 20 °C.

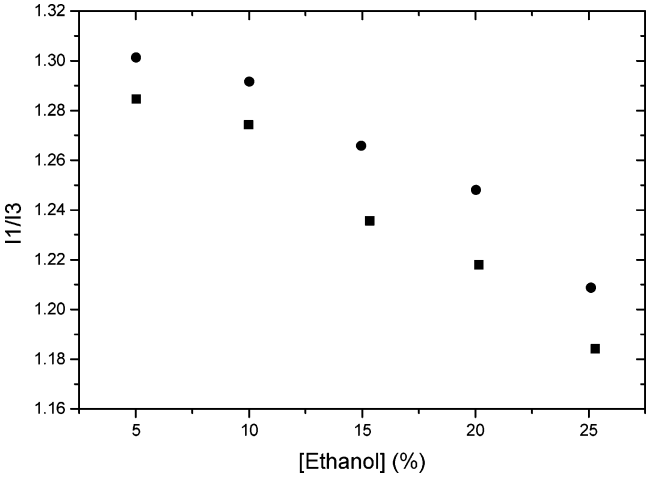

Figure 8. Polarity index (I_1/I_3) of pyrene in different water−ethanol mixtures in the presence of 25 g dm^{-3} of (■) $S_{15}E_{63}$ and (●) $E_{67}S_{15}E_{67}$.

adiabatic compressibility. Since the constitutive atomic volume of the block copolymer micelle may be assumed to be incompressible, the variations of β_S may be thought of as proceeding the sum of a positive intrinsic contribution (β_c) that reflects the imperfect packing of the copolymer chains and a negative hydration contribution (β_h) resulting from the interactions between the solute groups and the surrounding molecules,[54] $\beta_S = \beta_c + \beta_h$. On the basis of these definitions, two generalizations emerge. First, the tighter the internal packing of the core of the aggregate, the smaller its intrinsic compressibility and, consequently, the value of β_S. Second, the more polar groups that are exposed to the solvent, the more negative the hydration contribution and, consequently, the smaller the total value of β_S.

Figure 7 shows β_S as a function of copolymer $S_{15}E_{63}$ concentration at different ethanol concentrations in the mixed solvent. A similar picture was found for the triblock copolymer (not shown). As can be observed in this figure, the specific adiabatic compressibility increases with the ethanol content and remains practically constant with the copolymer concentration. This increment of β_S with the ethanol concentration in the solvent might arise from two different sources: On one hand, the mixed ethanol−water solvent is a better solvent for the copolymer due to the reduction of the interfacial tension between the mixed solvent and the polyoxyphenylethylene chains. This allows a less packed structure of the micelle core due to swelling of the hydrophobic S chains, which is reflected in an increase in β_c. The second factor arises from a decrease in β_h. This stems from the decrease in the aggregation number of the micelles and the presence of water molecules in the micellar core, which allows a slightly higher hydration of the hydrophobic blocks. However, a positive contribution to β_h may also exist. Molecular dynamics simulations[57] have demonstrated a very strong hydrogen-bonding interaction between the water molecules and the two lone pairs of oxygen atoms in the backbone of polyoxyethylene polymers. Thus, substitution of water molecules by ethanol ones with a lower ability to form hydrogen bonds will lead to a dehydration of the copolymer molecules and a subsequent increase in β_h.

Pyrene has been used as a probe to investigate the effect of ethanol on the core polarity of the micelles of the polyoxyphenylethylene−polyoxyethylene block copolymers. The relative intensity ratio of the first peak to the third peak within the vibrational bands of the pyrene emission spectrum has been shown to change with the local polarity of the surrounding environment of the probe molecules in a predictable fashion.[58] In the presence of micelles and other macromolecular systems, pyrene is preferentially solubilized in the inner hydrophobic regions of these associates. The I_1/I_3 ratio reflects the combined contributions of both the pyrene in the micelle cores and those in the solvent phase. Moreover, it is well-known that the I_1/I_3 ratio has a smaller value for pyrene in a hydrophobic environment in comparison to that in a hydrophilic one.[58−60]

Figure 8 shows the dependence of the I_1/I_3 ratio as a function of ethanol concentration in the mixed solvent for the diblock and triblock copolymers. As can be seen, the polarity sensed by pyrene decreases as the alcohol content increases for both copolymers in a nonlinear trend. This decrease can arise from the fact that solvent mixtures with increasing amounts of ethanol have a significantly higher capacity to accommodate pyrene molecules due to the lowering of solvent polarity, and thus, less pyrene molecules are solubilized in the micelle core. In this respect, it is worth mentioning that, with excitation of $\lambda = 339$ nm, the polarity sensed by pyrene in water solution was 1.51, whereas in ethanol it was 1.18,[61] in fair agreement with our values (1.53 and 1.17 for water and ethanol solutions, respectively; for our ethanol−water mixtures, we have obtained values of 1.51, 1.45, and 1.37 for 5, 15, and 25% (v/v) ethanol in the mixed solvent, respectively).

In contrast, a tentative explanation based only on an increase in solubilized pyrene in the micelle core as the ethanol content increases would not be supported: copolymer micelles decrease in size as the ethanol concentration in the solvent increases, and micelles with a smaller aggregation number have a more open structure, where a considerable contact between the inner regions of micelles and the surrounding solvent should take place due to the swelling of the polyoxyphenylethylene chains, which forces the probe to be located outside of the micelle. However, some solubilization must take place so the polarity index is lower than that in free ethanol solution.[62] In this respect, the polarity sensed by pyrene in the diblock copolymer micelle solution is lower than that in the triblock one as a consequence of the higher solubility of the probe in the core of the diblock micelles due to their higher size and larger relative hydrophobicity compared to that of the triblock.

4. Conclusions

In this work, we have analyzed how the presence of ethanol affects the micellization process of two structurally related polyoxyethylene block copolymers with diblock and triblock

architectures and the same hydrophobic block length, formed by oxyphenylethylene units. Surface tension data have shown that, in the case of the triblock, the cmc values increase as the ethanol content in the mixed solvent increases. The surface parameters show that the presence of ethanol involves the necessity of a larger space in the interface for the copolymer molecule. From light scattering data, it is derived that the block copolymers can be modeled as hard spheres, whose radii decrease as the ethanol concentration increases in solution, as also confirmed by transmission electron microscopy. Values of aggregation numbers decrease for a given copolymer as the ethanol content in the mixed solvent increases provided that mixed solvent becomes a better solvent for copolymer molecules. The addition of ethanol counterbalances the deswelling of the PEO chains due to a decrease of the water content and reduces the solvophobicity and increases the solubility of the S blocks, causing the lowering of the interfacial tension between the polyoxyphenylethylene core and the solvent and favoring the swelling of hydrophobic blocks. Therefore, to achieve thermodynamic equilibrium, the micelle size should be smaller. Moreover, this would indicate that micellar solvation is modified to some extent in magnitude with ethanol addition. In this respect, two aspects must be considered: first, the effect of steric character, since the ethanol molecule is larger than the water molecule, and, second, the consequence of the minor ability of ethanol to be a hydrogen-bond-forming molecule in relation to water. This is reflected in the compressibility data, for which their increment with ethanol content arises from the swelling of the hydrophobic polyoxyphenylethylene chains. Pyrene fluorescence data support the fact that copolymer micelles possess smaller aggregation numbers, having a more open structure, where a considerable contact between the inner regions of micelles and the surrounding solvent should take place due to the swelling of the polyoxyphyenylethylene chains, which forces the probe to be located outside of the micelle. However, some solubilization must take place so the polarity index is lower than that in free ethanol solution. Finally, the diblock copolymer seems to be slightly less altered in its micellar structure due to the presence of the alcohol as a consequence of a possible more compact structure of their micelle, as confirmed by light scattering, compressibility, and fluorescence data.

Acknowledgment. The project was supported by the Ministerio de Educación y Ciencia through project MAT2004-02756 and Xunta de Galicia. P.T. and E.C. thank Ministerio de Educación y Ciencia for his Ramón y Cajal position and his Ph.D. grant, respectively. We especially thank Professor Manuel Mosquera for the use of the fluorescence equipment and valuable discussions.

References and Notes

(1) Tuzar, Z.; Kratochvil, P. *Surface and Colloid Science*; Plenum Press: New York, 1993; Vol. 15.
(2) Alexandridis, P. *Curr. Opin. Colloid Interface Sci.* **1996**, *1*, 490.
(3) Martin, A.; Swarbrick, J.; Cammarata, A. *Physical Pharmacy*; Lea & Febiger Press: Philadelphia, PA, 1983.
(4) Kang, H. R. *J. Imaging Sci.* **1991**, *35*, 179.
(5) Feng, P.; Bu, X.; Pine, D. J. *Langmuir* **2000**, *16*, 5304.
(6) Alexandridis, P.; Holzwarth, J. F. *Langmuir* **1997**, *13*, 6074.
(7) Cheng, Y.; Jolicoeur, C. *Macromolecules* **1995**, *28*, 2665.
(8) Amstrong, J.; Chowdhry, B.; Mitchell, J.; Beezer, A.; Leharne, S. *J. Phys. Chem.* **1996**, *100*, 1738.
(9) Svensson, B.; Olsson, U.; Alexandridis, P. *Langmuir* **2000**, *16*, 6839.
(10) Ivanova, R.; Lindman, B.; Alexandridis, P. *Adv. Colloid Interface Sci.* **2001**, *89*−*90*, 351.
(11) Su, Y.; Wei, X.; Liu, H. *Langmuir* **2003**, *19*, 2995.
(12) Holmquist, P.; Alexandridis, P.; Lindman, B. *Langmuir* **1997**, *13*, 2471.
(13) Kelarakis, A.; Havredaki, V.; Booth, C. *Macromol. Chem. Phys.* **2004**, *205*, 1594.
(14) Pandit, N. K.; McIntyre, H. J. *Pharm. Dev. Technol.* **1997**, *2*, 181.
(15) Kwon, K. W.; Park, M. J.; Hwang, K. Char *Polym. J.* **2001**, *33*, 404.
(16) Alexandridis, P.; Yang, L. *Macromolecules* **2000**, *33*, 5574.
(17) Vadnere, M.; Amidon, G.; Lindenbaum, S.; Haslam, J. L. *Int. J. Pharm.* **1984**, *22*, 207.
(18) Ivanova, R.; Lindman, B.; Alexandridis, P. *Colloids Surf., A* **2001**, *183*−*185*, 41.
(19) Ivanova, R.; Alexandridis, P.; Lindman, B. *J. Colloid Interface Sci.* **2002**, *252*, 226.
(20) Deng, Y.; Price, C.; Booth, C. *Eur. Polym. J.* **1994**, *30*, 103.
(21) Crothers, M.; Attwood, D.; Collett, J. H.; Yang, Z.; Booth, C.; Taboada, P.; Mosquera, V.; Ricardo, N. P. S.; Martini, L. G. A. *Langmuir* **2002**, *18*, 8685.
(22) Yang, Z.; Crothers, M.; Ricardo, N. M. P. S.; Chaibundit, C.; Taboada, P.; Mosquera, V.; Kelarakis., A.; Havredaki, V.; Martini, L.; Valder, C.; Collett, J. H.; Attwood, D.; Heatley, F.; Booth, C. *Langmuir* **2003**, *19*, 943.
(23) Rekatas, C. J.; Mai, S.-H.; Crothers, M.; Quinn, M.; Collet, J. H.; Attwood, D.; Heatley, F.; Martini, L.; Booth, C. *Phys. Chem. Chem. Phys.* **2001**, *3*, 4769.
(24) Provencher, S. W. *Makromol. Chem.* **1979**, *180*, 201.
(25) El-Kashef, H. *Rev. Sci. Instrum.* **1998**, *69*, 1243. Lui. T.; Schuch, H.; Gerst, M.; Chu, B. *Macromolecules* **1999**, *32*, 6031. The temperature dependence of the Raleigh ratio was not found in the literature, and as a working approximation, values of R_v for toluene were adjusted relative to those published for benzene: Gulari, E.; Chu, B. *Biopolymers* **1999**, *32*, 2943. The adjustment is small over the temperature range involved.
(26) Mai, S.-M.; Ludhera, S.; Heatley, F.; Attwood, D.; Booth, C. *J. Chem. Soc., Faraday Trans.* **1998**, *94*, 567. Mai, S.-M.; Booth, C.; Kelarakis, A.; Havredaki , V.; Ryan, A. J. *Langmuir* **2000**, *16*, 1681.
(27) Harned, H. S.; Owen, B. B. *Physical Chemistry of Electrolyte Solutions*; Chapman and Hall: London, 1957; Chapter 8.
(28) Roux-Desgranges, G.; Bordere, S.; Roux, A. H. *J. Colloid Interface Sci.* **1994**, *162*, 284.
(29) Turro, N. J.; Yekta, A. *J. Am. Chem. Soc.* **1978**, *100*, 5958.
(30) Rosen, J. M.; Cohen, A. W.; Dahanakaye, M.; Hua, X. *J. Phys. Chem.* **1982**, *86*, 541.
(31) Sultana, S. B.; Bhat, S. G. T.; Rakshit, A. K. *Langmuir* **1997**, *13*, 4562.
(32) Evans, D. F.; Wennerström, H. *The Colloidal Domain: Where Physics, Chemistry and Biology Meet*; VCH: New York, 1994.
(33) Franks, F. In *Hydrogen Bonded Solvent Systems*; Covington, A., Jones, P. Eds.; Taylor and Francis: 1968.
(34) Marcus, Y. *Ion Solvation*; Wiley: London, 1985.
(35) Anad, K.; Yadav, O. P.; Singh, P. P. *Colloids Surf.* **1991**, *55*, 345.
(36) Vink, H. *J. Chem. Soc., Faraday Trans. 1* **1985**, *81*, 1725.
(37) Flory, P. J. *Principles of Polymer Chemistry*; Cornell UP: Ithaca, New York, 1953; p 532. For spheres, the excluded volume is 8 times the hard-sphere volume.
(38) Bronstein, L.; Chernyshov, D. M.; Timofeeva, G. I.; Dubrovina, L. V.; Valetsky, P. M.; Khokhlov, A. R. *J. Colloid Interface Sci.* **2000**, *230*, 140.
(39) Zheng, Y.; Won, Y.-Y.; Bates, F. S.; Davis, H. T.; Scriven, L. E.; Talmon, Y. *J. Phys. Chem. B* **1999**, *103*, 10331.
(40) Percus, J. K.; Yevick, G. J. *Phys. Rev.* **1958**, *110*, 1. Vrij, A. *J. Chem. Phys.* **1978**, *69*, 1742. Carnahan, N. F.; Starling, K. E. *J. Chem. Phys.* **1969**, *51*, 635.
(41) Solomon, M. J.; Müller, S. J. *J. Polym. Sci., Part B: Polym. Phys.* **1996**, *34*, 181.
(42) de Gans, B. J.; Kita, R.; Müller, B.; Wiegand, S. *J. Chem. Phys.* **2003**, *118*, 8073.
(43) Masegosa, R. M. Prolongo, M. G.; Hernández-Fuentes, I.; Horta, A. *Macromolecules* **1984**, *17*, 1181.
(44) Lin, Y.; Alexandridis, P. *Langmuir* **2002**, *18*, 4220.
(45) Yang, L.; Alexandridis, P. *Langmuir* **2000**, *16*, 4819.
(46) Mai, S.-M.; Booth, C.; Nace, V. M. *Eur. Polym. J.* **1997**, *33*, 991.
(47) Goldmints, I.; von Gottberg, F. K.; Smith, K. A.; Hatton, T. A. *Langmuir* **1997**, *13*, 3659.
(48) Liu, Y.; Chen, S. H.; Huang, J. S. *Macromolecules* **1998**, *31*, 2236.
(49) Pedersen, J. S.; Gerstenberg, M. C. *Colloids Surf., A* **2003**, *213*, 175.
(50) Castelletto, V.; Hamley, I. W. *J. Chem. Phys.* **2002**, *117*, 8124.
(51) Castelletto, V.; Hamley, I. W. *Langmuir* **2004**, *20*, 2992.
(52) Israelachvili, J. N. In *Physics of Amphiphiles: Micelles, Vesicles and Microemulsions*; Degiorgio, V., Corti, M., Eds.; North-Holland: Amsterdam, The Netherlands, 1985; Chapter 2.
(53) Gekko, K.; Noguchi, H. *J. Phys. Chem.* **1979**, *83*, 2706.
(54) Barbosa, S.; Castro, E.; Taboada, P.; Mosquera, V. *Mol. Phys.* **2005**, *103*, 2699.

(55) Chalikian, T. V.; Breslauer, K. *Proc. Natl. Acad. Sci.* **1996**, *93*, 1012.
(56) Barbosa, S.; Taboada, P.; Attwood, D.; Mosquera, V. *Langmuir* **2003**, *19*, 10200.
(57) Smith, G. D.; Bedrov, D. *J. Phys. Chem. B* **2003**, *107*, 3095.
(58) Kalyanusandaram, K.; Thomas, J. K. *J. Am. Chem. Soc.* **1977**, *99*, 2039.
(59) Itoh, H.; Ishido, S.; Nomura, M.; Hayakawa, T.; Mitaku, S. *J. Phys. Chem.* **1996**, *100*, 9047.
(60) Dong, D.; Winnik, M. A. *Can. J. Chem.* **1984**, *62*, 2560.
(61) Croy, S. R.; Kwon, G. S. *J. Controlled Release* **2004**, *95*, 161.
(62) Krueger, E.; Karpovich, D. S. Abstracts of Papers, 223rd ACS National Meeting, Orlando, FL, 2002.